


Research Article

# CircRNA\_MamI2 promotes the proliferation and migration of intestinal epithelial cells after severe burns by regulating the miR-93-3p/FZD7/Wnt/ $\beta$ -catenin pathway

Wenwen Zhang<sup>1,2,†</sup>, Yu Liao<sup>1,2,†</sup>, Jiaqi Lou<sup>1,2,†</sup>, Mengmeng Zhuang<sup>1,2,†</sup>, Hao Yan<sup>1,2</sup>, Qi Li<sup>1,2</sup>, Yuequ Deng<sup>1,2</sup>, Xiaohu Xu<sup>1,2</sup>, Dandan Wen<sup>1,2</sup> and Yong Sun<sup>1,2,\*</sup> 

<sup>1</sup>Department of Burn Surgery, the Affiliated Huaihai Hospital of Xuzhou Medical University, Xuzhou 221004, Jiangsu Province, China; and <sup>2</sup>Department of Burn Surgery, the 71st Group Army Hospital of PLA, Xuzhou 221004, Jiangsu Province, China

\*Correspondence. Email: sunyong\_97@163.com

<sup>†</sup>These authors contributed equally to this work.

Received 22 August 2021; Revised 8 February 2022; Editorial decision 10 February 2022

## Abstract

**Background:** Circular RNA (circRNA) plays key regulatory roles in the development of many diseases. However the biological functions and potential molecular mechanisms of circRNA in the injury and repair of intestinal mucosa in mice after severe burns are yet to be elucidated.

**Methods:** Cell counting kit-8 (CCK-8), 5-ethynyl-2'-deoxyuridine (EdU), wound healing and transwell assays were used to detect cell proliferation and migration ability. Real-time quantitative PCR was used to identify the expression of circRNA, microRNA and messenger RNA. Nuclear and cytoplasmic separation experiments were employed to perceive the location of circRNA\_MamI2. Finally, *in vitro* and *in vivo* experiments were conducted to study the repairing effect of circRNA\_MamI2 on the intestinal mucosa of mice after severe burns.

**Results:** When compared with the control group, the expression of circRNA\_MamI2 was significantly reduced in the severe burn group. Furthermore, overexpression of circRNA\_MamI2 promoted the proliferation and migration of CT26.wt cells *in vivo* and the repair of damaged intestinal mucosa *in vitro*. CircRNA\_MamI2 acted as a sponge adsorption molecule for miR-93-3p to enhance the expression of frizzled class receptor 7 and activate the downstream Wnt/ $\beta$ -catenin pathway, thereby promoting the repair of the intestinal mucosa.

**Conclusions:** Our findings demonstrate that circRNA\_MamI2 regulates the miR-93-3p/FZD7/Wnt/ $\beta$ -catenin pathway and promotes the repair of damaged intestinal mucosa. Hence, circRNA\_MamI2 is a potential therapeutic target to promote intestinal mucosal repair.

**Key words:** CircRNA\_MamI2, Severe burn, miR-93-3p, FZD7, Wnt/ $\beta$ -catenin pathway, Proliferation, Migration

## Highlights

- CircRNA\_Maml2 (circBase ID: mmu\_circ\_0015409) was significantly downregulated in the intestinal tissues of severely burned mice.
- CircRNA\_Maml2 regulates the miR-93-3p/FZD7/Wnt/ $\beta$ -catenin pathway to promote the repair of damaged intestinal mucosa.
- CircRNA\_Maml2 may become a potential molecular therapy target for patients with severe burns.

## Background

It is well known that burns not only cause damage to the skin surface but also inflict harm to the internal organs, especially the gastrointestinal mucosa [1]. Under normal circumstances, 30% of the body's circulating blood flows through the gastrointestinal tract. When the body suffers severe burns or shock, the blood flow is redistributed throughout the body to protect the heart, brain and other important organs. Hence, gastrointestinal blood flow is reduced, resulting in intestinal barrier dysfunction [2,3]. At such times, the intestinal microflora is displaced, leading to intestinal infection, intestinal shock, systemic inflammatory syndrome and even multiple organ dysfunction syndromes [4,5]. Therefore, it is imperative to clarify the underlying mechanism of the pathogenesis of intestinal mucosal injury and repair after severe burns, and to develop effective therapeutic approaches for damaged intestinal mucosa.

Circular RNA (circRNA) is a novel endogenous non-coding RNA with a length ranging from several hundred to several thousand base pairs. The closed loop is formed by the covalent bond between the 5' and 3' ends [6]. CircRNA was discovered by Sanger *et al.* in infected plant species over 40 years ago [7]. At that time, it was thought to be caused by incorrect splicing and was presumed to have no function [8]. With the development of biological information technology and the continuous progress of sequencing technology, more and more circRNAs were discovered and became the focus of research. Since circRNA has no 5' end-cap structure and 3' poly (A) tail, and is more stable than linear RNA. Furthermore, it can resist digestion by RNase R and can exist stably in the circular form, which makes it a molecular therapeutic target in a variety of diseases [9,10]. In previous studies, several abnormally expressed circRNAs have been found in the intestinal tissues of severely burned mice, of which circRNA\_Maml2 (mmu\_circRNA\_43775, circBase ID: mmu\_circ\_0015409) was most significantly downregulated [11]. circRNA\_Maml2, which originates from the messenger RNA (mRNA) trans-splicing of Maml2 and is formed by the second ring of five exons, is located on chromosome 9 (13619989–13 621 675) and is 1686 bp in length. However, the role of circRNA\_Maml2 in the repair of intestinal mucosal damage after severe burns remains unclear.

### MicroRNA

(miRNA) is also a non-coding single-stranded RNA present in the genome of higher eukaryotes, which has been identified in recent years. miRNA is composed of ~22 nucleotides and plays a post-transcriptional regulatory role in gene

expression. The human genome contains numerous miRNAs. It is estimated that miRNAs can control >60% of the activity of all protein-coding genes and participate in the regulation of almost every cellular process studied thus far. Although the sequence of miRNA is not long, the functions of the 5'- and 3'-terminals are different. The 5'-terminal is related to the recognition of mRNA, while the 3'-terminal is linked to the structural stability of biological macromolecules [12]. The nucleotides at positions 2 and 8 at the end of miRNA are called seed regions. It has been reported that non-coding RNA, including circRNA, long non-coding RNA and pseudogenes, can competitively bind to the miRNA response element (MRE) to interact with and regulate each other. This constitutes the competitive endogenous RNA (ceRNA) hypothesis [13]. At the same time, the seed sequence of miRNAs can also be completely or incompletely complementary to the 3' untranslated region (UTR) of target gene mRNA, and finally play a regulatory role by degrading mRNA or inhibiting the protein synthesis [14]. The most classic example is CDR1as/ciRS-7, which contains dozens of binding sites to miR-7 and significantly inhibits its activity, thus raising the level of miR-7 target genes and further exerting biological effects [15]. However, the mechanism by which circRNA\_Maml2 promotes intestinal mucosal repair is unclear.

In this study, we first confirmed that circRNA\_Maml2 decreased significantly in the intestines of severely burned mice. Then, we found that overexpression of circRNA\_Maml2 could promote cell proliferation and migration *in vitro* and stimulate the repair of damaged intestinal mucosa *in vivo*. In terms of a regulatory mechanism, circRNA\_Maml2 can be used as a sponge molecule of miR-93-3p, thus targeting to regulate the expression level of frizzled class receptor 7 (FZD7). In turn, FZD7 acts as the receptor of the Wnt pathway, and the combination of FZD7 and miR-93-3p can activate the Wnt/ $\beta$ -catenin star pathway and further promote the repair of the intestinal mucosa. In short, circRNA\_Maml2 may serve as a molecular biological target for treatment of the intestinal mucosa after severe burns.

## Methods

### Cell culture

Mouse CT26.wt cell line was purchased from American Type Culture Collection (ATCC, USA). The cell line was cultured in RPMI1640 medium supplemented with 10% fetal bovine serum (ExCell Bio, China, Uruguay Origin) and 1% penicillin,

streptomycin and amphotericin-B. All cells were incubated in a constant temperature incubator maintained at 37°C and containing 5% CO<sub>2</sub>.

#### Vector construction and cell transfection

To overexpress circRNA\_Maml2, circRNA\_Maml2 cDNA was synthesized and cloned into pAdEasy-EF1-MCS-CMV-GFP (EcoRI MCS) vector, which includes anterior and posterior circular frames. As the control, the empty vector did not have the sequence of circRNA\_Maml2. The plasmid was transfected into HEK-293A cells according to the instructions for the Lipofiter™ transfection reagent, and the adenovirus (Ad) was packaged using the Adeasy adenovirus system. *Escherichia coli* DH5- $\alpha$  was used to amplify the adenovirus vector and auxiliary packaging vector plasmid. The packaging of the adenovirus was completed by Hanbio Biotechnology Co. Ltd (Shanghai, China). The miR-93-3p mimic was designed and synthesized by Gene-Pharma (Shanghai, China). Oligonucleotides were transfected into CT26.wt cells using X-treme (Sigma, USA) according to the manufacturer's instructions. The efficiency of silencing and overexpression was detected by quantitative real-time polymerase chain reaction (qRT-PCR).

#### RNA extraction, RNase R treatment and qRT-PCR

TRNzol Universal Reagent (TIANGEN, China) was used to isolate the total RNA from the tissues and cells according to the manufacturer's protocol. Genomic DNA (gDNA) was extracted by the method prescribed by Tiangen Biochemical Technology (Beijing) Co. Ltd. RNase R treatment solution was incubated at 37°C with 1 U/ $\mu$ g of RNase R (Epicenter, WI, USA) for 15 min based on the manufacturer's protocol. For circRNA and mRNA, cDNA was synthesized using the PrimeScript™ RT reagent kit with the gDNA Eraser (TaKaRa, Japan) as per the manufacturer's instructions. Then the expression of circRNA and mRNA was detected by qRT-PCR according to the manufacturer's instructions (TB Green® Premix Ex Taq™II (Tli RNaseH Plus) TaKaRa, Japan). For miRNA, cDNA was synthesized by cDNA using the First Chain Synthesis Kit (TIANGEN, China) according to the given protocol. Subsequently, qRT-PCR was carried out using the 7500 Real-time PCR System (Thermo Fisher Scientific, USA) to detect the level of miRNA with an miRcute enhanced miRNA Fluorescence Quantitative Detection Kit (SYBR Green, TIANGEN, China). Glyceraldehyde-3-phosphate dehydrogenase (*Gapdh*) and U6 small nuclear RNA (*U6*) acted as the internal references of circRNA, mRNA and miRNA. All primers were synthesized by Sangon Biotech (Shanghai, China). All data were analyzed by the 2<sup>- $\Delta\Delta$ Ct</sup> method. The primer details are as follows: *Gapdh* F: 5'-TTCAACGGCACAGTCAAG-3'; *Gapdh* R: 5'-CACCCATTGATGTTAGTG-3'; circRNA\_Maml2 F: 5'-AGCAGCAGCAGCAACCATCG-3'; circRNA\_Maml2 R: 5'-CAAAGAGCCCTGGAGCTGTCTG-3'; *U6* F: 5'-CCTGCTTCGGCAGCAC-3'; miR-93-3p F: 5'-CCACTGCTGAGCTAGCACTTCCCG-3'; *Fzd7* F: 5'-CTTT

GTGTCTCTCTTTTCGCATC-3'; *Fzd7* R: 5'-CTCATAAAAGTAGCAGGCCAAC-3'.

#### Cell proliferation assay

Cell counting kit-8 (CCK-8) assay and 5-ethynyl-2'-deoxyuridine (EdU) assays were used to detect cell proliferation. For the CCK-8 assay, the transfected CT26.wt cells were inoculated in a 96-well plate at a density of 5 × 10<sup>3</sup> cells/well. Cell proliferation was measured using the CCK-8 (Dojindo Laboratories, Kumamoto, Japan) as per the instructions, and then the absorbance at the 450 nm for each well was detected spectrophotometrically (Bio-Rad, USA) at 0, 24, 48 and 72 h. For the EdU assay, the transfected CT26.wt cells were seeded in a 96-well plate at a density of 5 × 10<sup>3</sup> cells/well, while the proliferation viability of the cells in each well was evaluated using the Cell-Light™ EdU Apollo567 In Vitro Kit (RiboBio, Guangzhou, China) according to the manufacturer's protocol. All images were photographed and saved using an inverted fluorescence microscope (Olympus, Japan), and the ratio of EdU-stained cells to Hoechst-stained cells was calculated to evaluate cell proliferation.

#### Cell migration assay

The migration ability of CT26.wt cells was detected by wound healing and transwell assays. For wound healing assays, the transfected CT26.wt cells were seeded in a 6-well plate and cultured until they reached 100% confluence. A straight artificial wound was then drawn with a 1000- $\mu$ l pipette tip. The images of wound healing at 0 and 24 h were obtained using a microscope (Olympus, Japan). For the transwell migration assay, the transfected cells were seeded in the upper chamber containing 100- $\mu$ l of serum-free basal medium, and the lower chamber contained 600  $\mu$ l of complete medium with 20% serum. The cells were incubated for 24 h, fixed with formaldehyde and stained with 0.5% crystal violet staining solution for 20 min. The cells in the upper chamber were gently wiped with a cotton swab. Finally, the images of cell migration were obtained microscopically (Olympus, Japan).

#### Nuclear and cytoplasmic separation experiment

When CT26.wt cells had reached 100% confluence, the cells were collected and nuclear-cytoplasmic separation was performed using the Minute™ Cytoplasmic and Nuclear Isolation Kit (Invent Biotechnologies, Inc., MN, USA) according to the manufacturer's protocol. The RNA was then extracted from the nucleus and the cytoplasm by the TRNzol method, and qRT-PCR was used to detect the expression of circRNA\_Maml2 in the nucleus and cytoplasm. *U6* and *Gapdh* were used as internal controls for the nucleus and cytoplasm, respectively.

#### RNA fluorescence *in situ* hybridization assay

Fluorescence *in situ* hybridization (FISH) was performed using the fluorescence *in situ* hybridization kit (RiboBio,

Guangzhou, China) to study the distribution of circRNA\_Maml2 in the CT26 cells. The hybridization was conducted overnight with a Cy3-labeled circRNA\_Maml2 probe and mmu-miR-93-3p probe. All images were captured by a Nikon A1Si Laser Scanning Confocal Microscope (Nikon Instruments Inc., Japan).

#### Pull-down assay and qRT-PCR

To test and verify the direct binding between circRNA\_Maml2 and miRNAs, an RNA pull-down assay with MS2-binding protein (MS2bp) was performed, which specifically binds RNA containing MS2-binding sequences (MS2bs), to pull down endogenous miRNAs or proteins associated with circRNA\_Maml2. We generated a construct containing circRNA\_Maml2 transcript combined with MS2bs elements (named MS2bs circRNA\_Maml2) and co-transfected it into CT26.wt cells with a construct containing MS2bp-FLAG. Immunoprecipitation was then performed using FLAG antibody, and IgG was used as a negative control. The RNA products were analyzed by qRT-PCR.

#### Luciferase reporter assay

The plasmid containing circRNA\_Maml2 wild-type (pSI-Check2-circRNA\_Maml2-wt) and mutant (pSI-Check2-circRNA\_Maml2-mut) sequences were synthesized, and the plasmid and miR-93-3p mimic were co-transfected into CT26.WT cells using the Lipofectamine 2000 reagent (Invitrogen, CA, USA). Finally, the luciferase activity of fireflies was measured by the dual luciferase reporter gene detection kit (Beyotime, Shanghai, China).

#### Western blotting analysis

The total protein in the CT26.wt cells was extracted with radioimmunoprecipitation assay lysate and phenylmethylsulfonyl fluoride protease inhibitor (VICMED, Jiangsu, China), and its concentration was determined by the bicinchoninic acid protein assay kit (Beyotime, Shanghai, China). The proteins were separated using 10% sodium dodecyl sulfate polyacrylamide gel electrophoresis (Sangon Biotech, Shanghai, China) and then electrically transferred to a polyvinylidene fluoride membrane (Millipore, MA, USA). The membrane was sealed with 5% skimmed milk powder at room temperature for 2 h and then incubated with the primary antibody dilution at 4°C overnight. On the second day, the membrane was washed thrice with Tris-buffered saline with 0.1% Tween-20 detergent and then incubated with the secondary antibody diluent at room temperature for 2 h. Finally, the bolt signal was visualized by a chemiluminescence gel imaging system (Tanon, Shanghai, China) with an electrochemiluminescence substrate (Bioworld, USA).

#### Mouse model of third-degree burn and sample collection

A burn model of normal healthy adult C57BL/6 J mice was constructed [16]. The project was examined and

verified by the Laboratory Animal Ethics Committee Xuzhou Medical University in accordance with the Guide to Laboratory Animal Ethics Examination of Xuzhou Medical University. The relevant animal experiments were permitted. The process number for animal experiments was: 202010 W001. After weighing the mice, they were divided into three groups according to the random number method: control group (C group,  $n=10$ ), burn group (B group,  $n=10$ ) and Ad-circRNA\_Maml2 + burn group (Ad-circRNA\_Maml2 + burn,  $n=10$ ; the mice were injected via gastric lavage with 10  $\mu\text{L/g}$  circRNA\_Maml2 30 min before scalding). Then, 1% pentobarbital sodium (0.1 mL/10 g) was injected intraperitoneally, the back was depilated with scissors and 8% sodium sulfate, after which the back was placed in boiling water (100°C) for 10 s, resulting in 30% third-degree scalding. Buprenorphine (0.1 mg/kg) was injected intraperitoneally to minimize the pain of the animals [17], 1 mL of lactic acid green sodium (50 mL/kg) was injected into the abdominal cavity for anti-shock treatment immediately, and iodophor was applied to the back for anti-infection and covered with gauze for insulation. The whole layer of skin injury was confirmed by pathological sectioning. A false scald control model was produced as follows: the mice were anesthetized and depilated according to the method described above, and their backs were exposed to warm water (37°C) for 10 s. After 24 h, the intestinal tissues in the severe burn group (B group), Ad-circRNA\_Maml2 + burn group (Ad-circRNA\_Maml2 + burn group) and control group (C group) were collected 5 cm above the ileocecal area. After the tissue sample was isolated, the intestinal tube was cleaned with pre-cooled phosphate-buffered saline. As soon as possible after, the filter paper was soaked dry, the intestinal tissue was wrapped in a 2-mL Eppendorf tube with tin foil, placed in a liquid nitrogen tank for rapid freezing and stored at  $-80^{\circ}\text{C}$ . To reduce the occurrence of RNA degradation, the time interval from *in vitro* to placing the sample in liquid nitrogen should not exceed 10 min. A part of the sample was stored in the refrigerator at  $-80^{\circ}\text{C}$ . A small number of the samples were observed under light microscopy to observe the morphology of the intestinal mucosa according to the colonic mucosa damage index (CMDI) (Table 1). The other part of the sample was fixed in 4% paraformaldehyde for hematoxylin and eosin (HE) staining, and the pathological changes in the intestinal tissues were scored according to Chiu's scoring criteria (Table 2). Meanwhile, we collected blood from the eyeballs, centrifuged it at 3000g/4°C for 10 min, stored the serum in a refrigerator at  $-80^{\circ}\text{C}$  and determined the diamine oxidase (DAO) content in the serum by using an ultraviolet spectrophotometer (Bio-Rad, USA) [18].

#### Human experiments

Colonoscopy biopsy specimens of the intestinal mucosa tissues of eight patients with severe burns who visited the Burns Department of the Huaihai Hospital Affiliated to Xuzhou Medical University from August 2019 to December 2020

**Table 1.** Evaluation of macroscopic scores

Score	Colon damage
0	No damage
1	Modest hyperemia and edema without ulcers.
2	Hyperemia and edema, with rough and granular mucosa.
3	Serious hyperemia and edema with necrosis and ulcer formation with ulcer diameter < 1 cm with necrotic inflammation.
4	Maximum longitudinal diameter of the ulcer is >1 cm or full-length wall necrosis on the basis of three points.

**Table 2.** Evaluation of microscope scores

Score	Grade	Standard
1	0	Normal intestinal villi.
2	1	Capillary apical villi with capillary congestion.
3	2	Extension of the submucosal space and separation of intestinal mucosa and submucosa.
4	3	Massive epithelial falling off.
5	4	Separation complete of the epithelium, with only the lamina propria left.
6	5	Digestion of the lamina propria, hemorrhage and ulceration.

were collected. Eight normal intestinal mucosa specimens were obtained from healthy volunteers. The specimens were stored in liquid nitrogen. This study was approved by the Medical Theory Committee of the Huaihai Hospital Affiliated with Xuzhou Medical University. All patients provided their informed consent. We performed PCR on the damaged intestinal mucosa specimens and normal intestinal mucosa specimens to detect the expression level of circRNA\_Maml2.

### Statistical analysis

The data were analyzed by SPSS 22.0 (IBM, SPSS, Chicago, IL, USA) and plotted by GraphPad Prism 8.0 (GraphPad Software Inc., CA, USA). The data are expressed as mean  $\pm$  standard deviation (mean  $\pm$  SD). The experiment was conducted  $\geq 3$  times. Student's *t*-test was used between the two groups and one-way analysis of variance was used between multiple groups.  $P < 0.05$  was considered statistically significant. Because there are two different groups of data at different times in this experiment, it is necessary to analyze the influence of both processing factors and time factors on the experimental results. The statistical method used at this time is the repeated measures analysis of variance. This study was a study with a small sample size (<50 cases), so the Shapiro–Wilk method was used to test normality. When  $p > 0.05$ , it was considered to be normally distributed.

## Results

### Expression level and source of circRNA\_Maml2 in intestinal tissues of mice after severe burn

To detect the expression level of circRNA\_maml2 in the intestinal mucosa we constructed a burn mouse model. The results signified that circRNA\_Maml2 was most obviously and prominently downregulated in burn mouse model

intestinal samples, which attracted our attention (Figure 1a). According to circBase data (<http://www.circbase.org/>), circRNA\_Maml2 was derived from exon 2 of Maml2 on chromosome 9 and then formed a 1686 nt circular transcript (Figure 1b). Next, we chose CT26.wt cells to explore the function and regulation of circRNA\_Maml2.

### Identification of circRNA\_Maml2 ring structure and location experiment

To further confirm that circRNA\_Maml2 is a circular transcript, we designed specific back-to-back primers and face-to-face primers for the sequence of circRNA\_Maml2. Then the gene was amplified by qRT-PCR and the cyclization site was confirmed by Sanger sequencing. The results indicated that circRNA\_Maml2 could be amplified in cDNA and not in the gDNA (Figure 2a). With regard to the detection of circRNA\_Maml2 stability, the total RNA was extracted and treated in the presence and absence of RNase R. The results demonstrated that the expression level of linear Maml2 mRNA decreased significantly after RNase R treatment; however, the expression level of circRNA\_Maml2 did not change significantly (Figure 2b). This finding reveals that the annular circRNA\_Maml2 was more stable than its linear Maml2 mRNA. We then performed nuclear and cytoplasmic separation experiments and RNA FISH assay to discern the location of circRNA\_Maml2 in the CT26.wt cells and found them to be mainly distributed in the cytoplasm (Figure 2c, d).

### CircRNA\_Maml2 promotes CT26.wt cell proliferation and migration

To decipher the function of circRNA\_Maml2 in the CT26.wt cells, we constructed an adenovirus overexpression vector



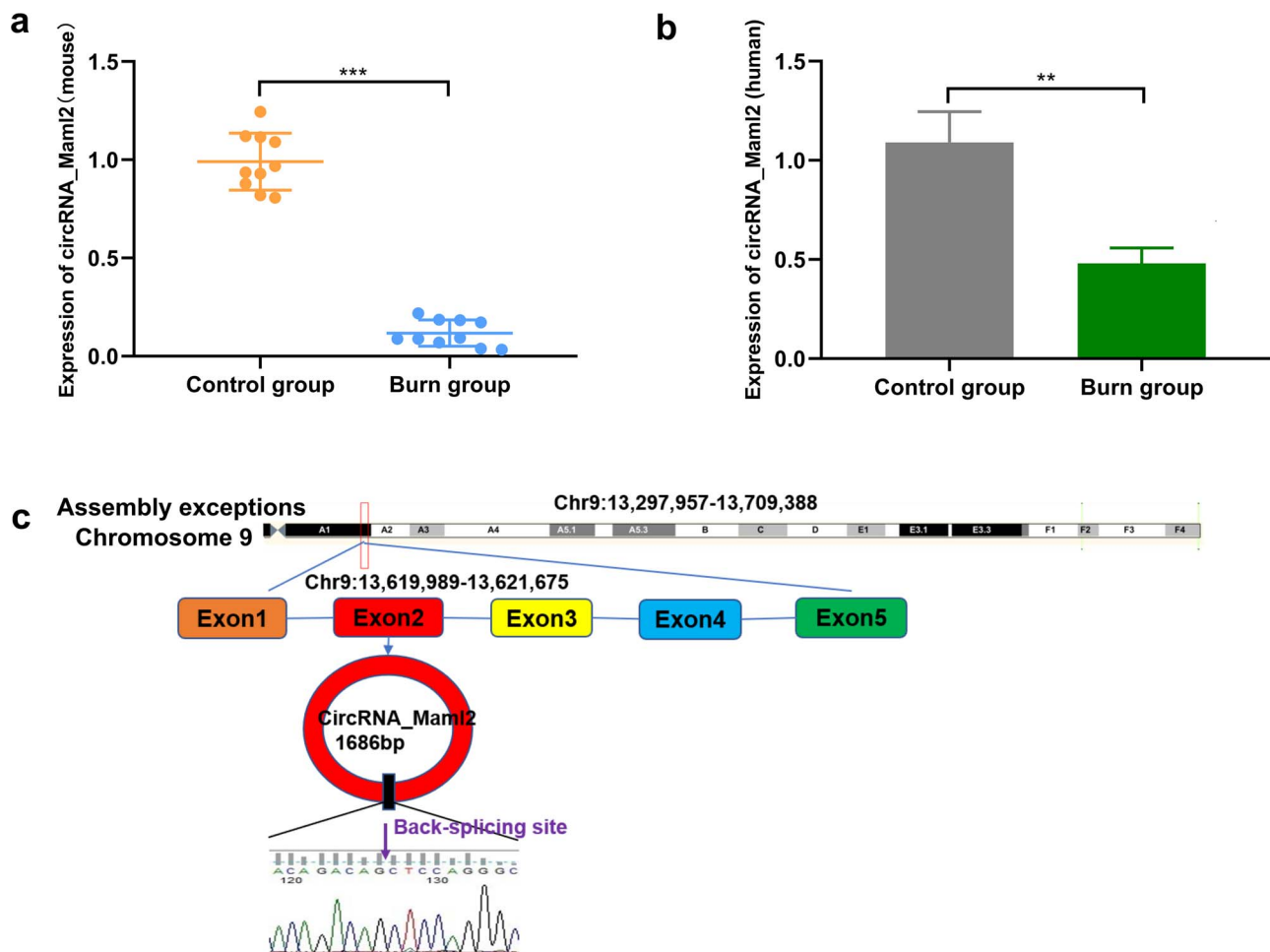


**Figure 1.** Expression level and schematic diagram of circRNA\_Maml2. (a) Expression level of circRNA\_Maml2 after severe burn (mouse sample). (b) Expression level of circRNA\_Maml2 after severe burn (human sample). (c) Schematic diagram of circRNA\_Maml2 loop formation; \*\* $p < 0.01$ , \*\*\* $p < 0.001$

**Table 3.** Details of five miRNAs

miRNA name	miRNA sequence	Seed location	Number of binding sites
miR-6400	UUCUUGCUGCUUGGUGCUCGC	AGCAAGA	5
miR-683	CCUGCUGUAAGCUGUGUCCUC	ACAGCAG	9
miR-367-5p	ACUGUUGCUAACAUGCAACUC	GCAACAGA	7
miR-7117-5p	UCUGGGGGCUCAGCUGAGGAUA	CCCCCAG	4
miR-93-3p	ACUGCUGAGCUAGCACUCCCCG	TCAGCAG	4

specific to circRNA\_Maml2 and observed that the vector could stably increase the expression of circRNA\_Maml2 in the CT26.wt cell lines (Figure 3a). Moreover, we noted that the overexpression of circRNA\_Maml2 did not change the expression level of linear Maml2 mRNA (Figure 3b). Then, we examined the effect of circRNA\_Maml2 on cell proliferation. The results of the CCK-8 assay showed that up-regulation of circRNA\_Maml2 promoted cell proliferation (Figure 3c). The results of the EdU assay disclosed that up-regulation of circRNA\_Maml2 significantly increased the number of EdU-positive cells (Figure 3d). Furthermore, we performed wound healing and transwell analyses to explore

the effect of circRNA\_Maml2 on the migration ability of CT26.wt cells. The results of the wound healing experiment suggested that the overexpression of circRNA\_Maml2 could significantly promote wound healing (Figure 3e). The results of the transwell experiment indicated that the overexpression of circRNA\_Maml2 could significantly enhance cell migration (Figure 3f).

#### CircRNA\_Maml2 acts as a sponge for miR-93-3p

To further elucidate the regulatory mechanism of circRNA\_Maml2, we used Targetscan and miRanda prediction software to predict the potential targets of circRNA\_Maml2.

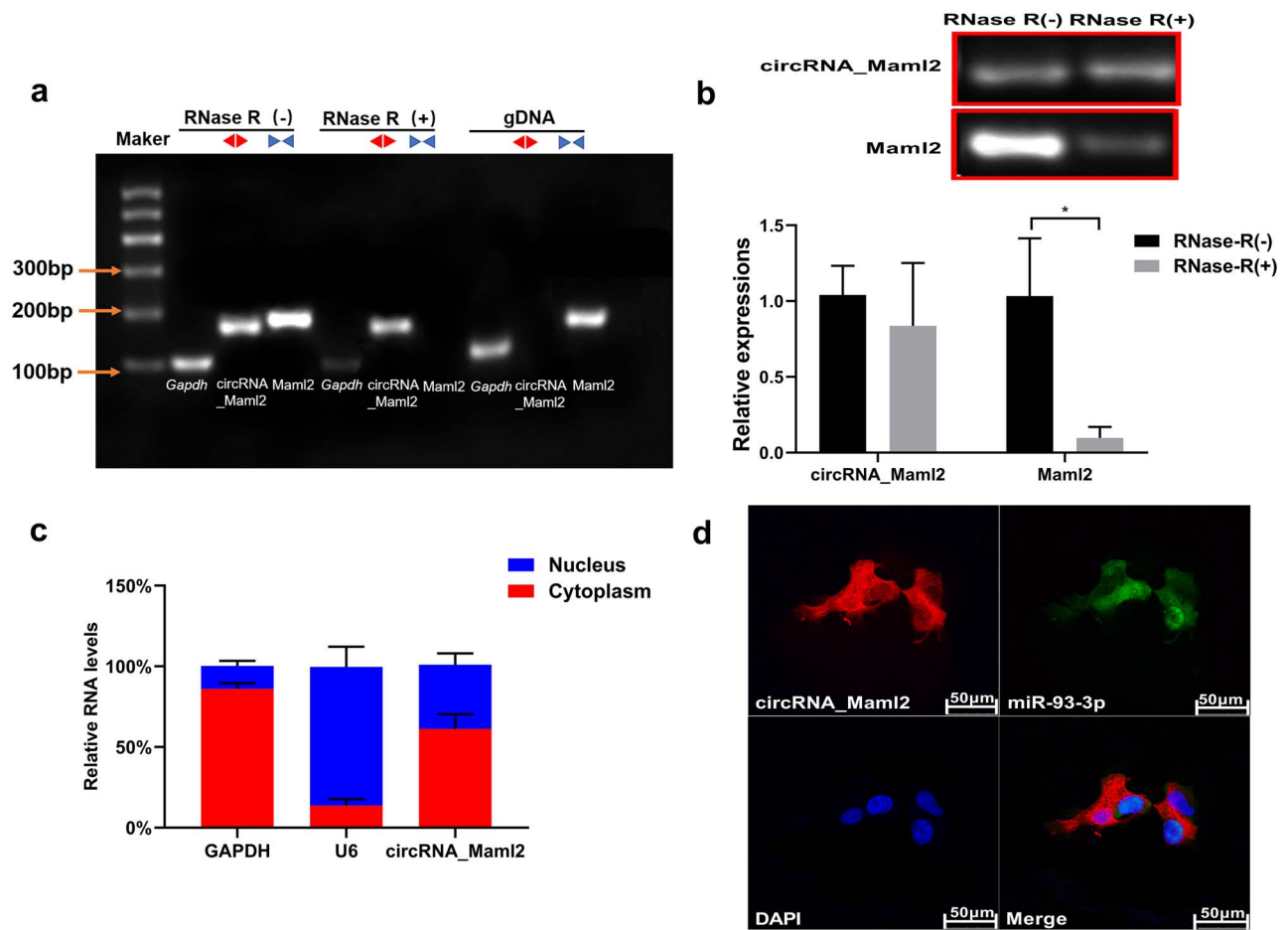


**Figure 2.** Identification of circRNA\_Maml2 ring structure and location experiment. (a) The existence of circRNA\_Maml2 in CT26.wt cells verified by RT-PCR. Different primers can amplify circRNA\_Maml2 in cDNA but not genomic DNA (gDNA). *Gapdh* was used as the linearity control. (b) After RNase R treatment, the relative expressions of circRNA\_Maml2 and Maml2 in CT26.wt cells were measured by qRT-PCR assay. (c) The abundance of circRNA\_Maml2 in either the cytoplasm or nucleus of CT26.wt cells detected by qRT-PCR. \* $p < 0.05$ . (d) FISH was performed to observe the cellular location of circRNA\_Maml2 (red) and nucleus (green) in cells (magnification  $\times 200$ , scale bar =  $50 \mu\text{m}$ ). *GAPDH* Glyceraldehyde-3-phosphate dehydrogenase, *qRT-PCR* quantitative real-time polymerase chain reaction, *FISH* fluorescence in situ hybridization

After calculating their intersection, we identified five potential binding miRNAs, namely miR-6400, miR-683, miR-367-5p, miR-7117-5p and miR-93-3p (Table 3), among which the one with the highest score and more conservative target site was miR-93-3p. The qRT-PCR results indicated that the expressions levels of miR-93-3p and miR-683 were reduced, while the expression level of miR-93-3p was significantly lowered after the overexpression of circRNA\_Maml2, while the other three miRNAs exhibited different trends (Figure 4a). At the same time, we perceived that the expression of miR-93-3p was elevated in the intestinal tissue of severely burned mice (Figure 4b). Then, to understand the interaction between circRNA\_Maml2 and miR-93-3p, we conducted a pull-down experiment to evaluate whether circRNA\_Maml2 can directly capture miR-93-3p. The results showed that circRNA\_Maml2 with a specific biotinylated MS2 tag could indeed capture a large amount of miR-93-3p (Figure 4c). As the immediate next step, we performed a dual luciferase reporter gene test. The results showed that the miR-93-3p mimic significantly inhibited the activity of the

wild-type circRNA\_Maml2 luciferase reporter but failed to inhibit the activity of the mutant type circRNA\_Maml2 luciferase reporter (Figure 4d). This finding indicated that there may be a direct interaction between circRNA\_Maml2 and miR-93-3p through complementary binding sequences. These results strongly suggest that circRNA\_Maml2 acts as a sponge molecule for miR-93-3p.

#### MiR-93-3p inhibits cell proliferation and migration by targeting *Fzd7*

Studies have reported that miR-93-3p can inhibit cell proliferation and migration [19–21]. The expression of miR-93-3p was upregulated after transfection of the miR-93-3p mimic into the CT26.wt cells (Figure 5a). The results of the CCK-8 analysis confirmed that the proliferation ability of cells was obviously inhibited because of the up-regulation of miR-93-3p (Figure 5b). The EdU experiment indicated that the proliferation rate of EdU-positive cells was significantly compromised owing to the up-regulation of miR-93-3p

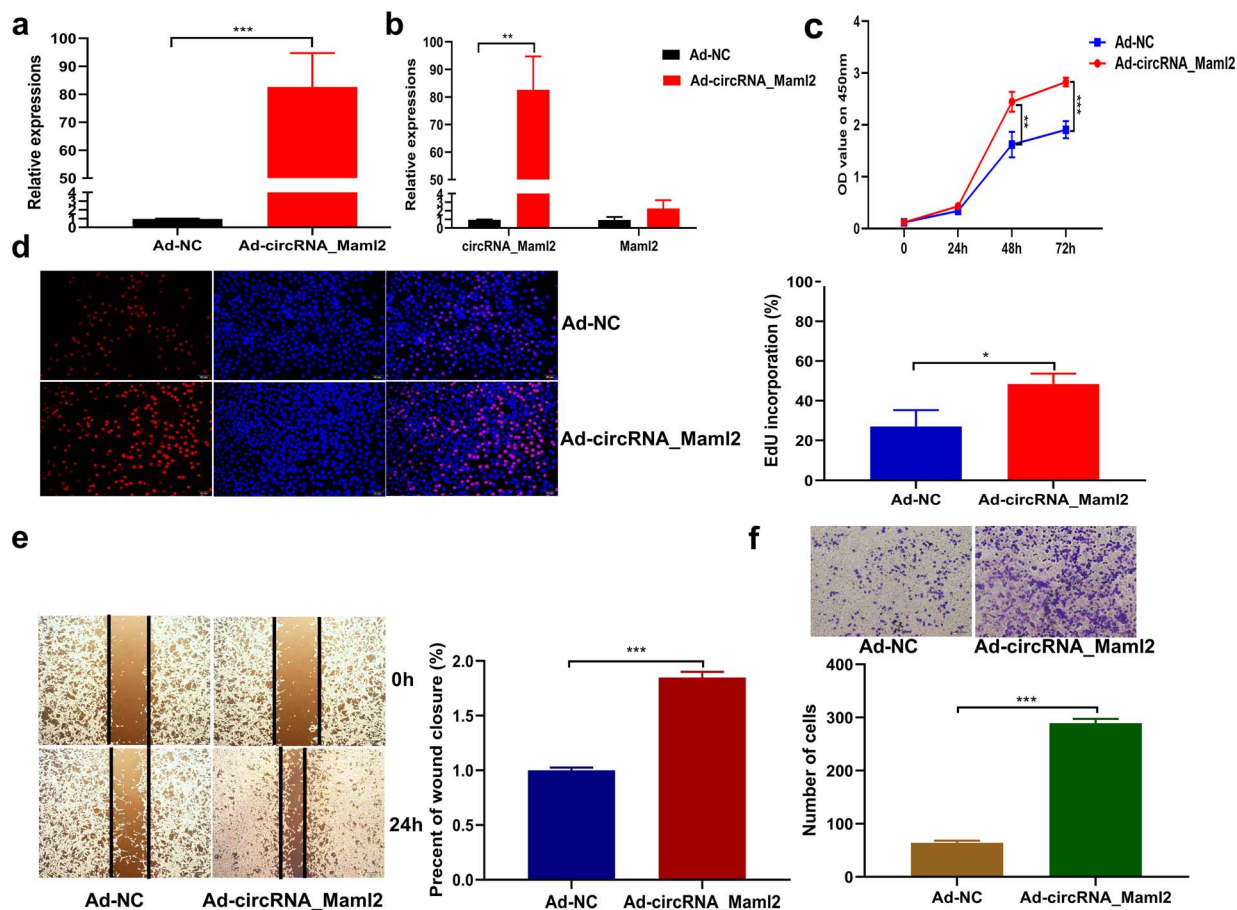


**Figure 3.** CircRNA\_Maml2 promotes cell proliferation and migration. (a) qRT-PCR assay was conducted to verify the expression of circRNA\_Maml2 in CT26.wt cells transfected with overexpression of adenovirus targeting circRNA\_Maml2. (b) Linear mRNA expression of Maml2 after transfection with overexpression of adenovirus targeting circRNA\_Maml2. (c) Growth curves of CT26.wt cells transfected with Ad-circRNA\_Maml2 detected by the CCK-8 assay. (d) Number of EdU-positive CT26.wt cells transfected with Ad-circRNA\_Maml2 detected by the EdU assay. (e, f) The migration ability of CT26.wt cells transfected with Ad-circRNA\_Maml2 was detected by a wound healing experiment and transwell experiment. \* $p < 0.05$ , \*\* $p < 0.01$ , \*\*\* $p < 0.001$ . Ad adenovirus, CCK-8 cell counting kit-8, EdU 5-ethynyl-2'-deoxyuridine, GAPDH glyceraldehyde-3-phosphate dehydrogenase, qRT-PCR quantitative real-time polymerase chain reaction

(Figure 5c). The results of the wound healing and transwell experiments disclosed that the migration ability of cells was very much inhibited by the up-regulation of miR-93-3p (Figure 5d, e). miRNA can bind to the 3'-UTR of the mRNA through the seed sequence to either degrade or inhibit the translation of the target protein. TargetsCan and miRDB prediction software were used to decipher the potential targets of miR-93-3p. According to the scores, *Fzd7*, *Arf4*, *Pbf6* (PHD finger protein 6) and *Smad2* (SMAD family member 2) were chosen as the potential target gene of miR-93-3p. Then, the miR-93-3p mimic was again transfected into the CT26.wt cells, and the results indicated that the mimic significantly inhibited *Fzd7* mRNA and protein expression levels, whereas *Arf4* and *Pbf6* demonstrated an upward trend, while the expression level of *Smad2* did not change significantly (Figure 5f, g). To further prove that *Fzd7* is the target of miR-93-3p, the wild-type or mutant sequence of *Fzd7* 3'-UTR containing miR-93-3p

binding sequence was used to synthesize the luciferase reporter plasmid. Analysis of the luciferase reporter results suggested that the co-transfection of miR-93-3p mimic and *Fzd7* wild-type plasmid significantly reduced luciferase activity. However, co-transfection of miR-93-3p mimic and *Fzd7* mutant plasmid did not alter the luciferase activity (Figure 5i). In addition, we also observed that the expression of *Fzd7* in the intestinal tissue of severely burned mice was reduced (Figure 5h).

#### CircRNA\_Maml2 indirectly regulates FZD7 through miR-93-3p

In CT26.wt cells, we found that *Fzd7* mRNA and protein expression levels increased after the over-expression of circRNA\_Maml2, while they decreased after the up-regulation of miR-93-3p (Figure 6a, b). Therefore, as expected, the up-regulation of *Fzd7* caused by the over-expression of



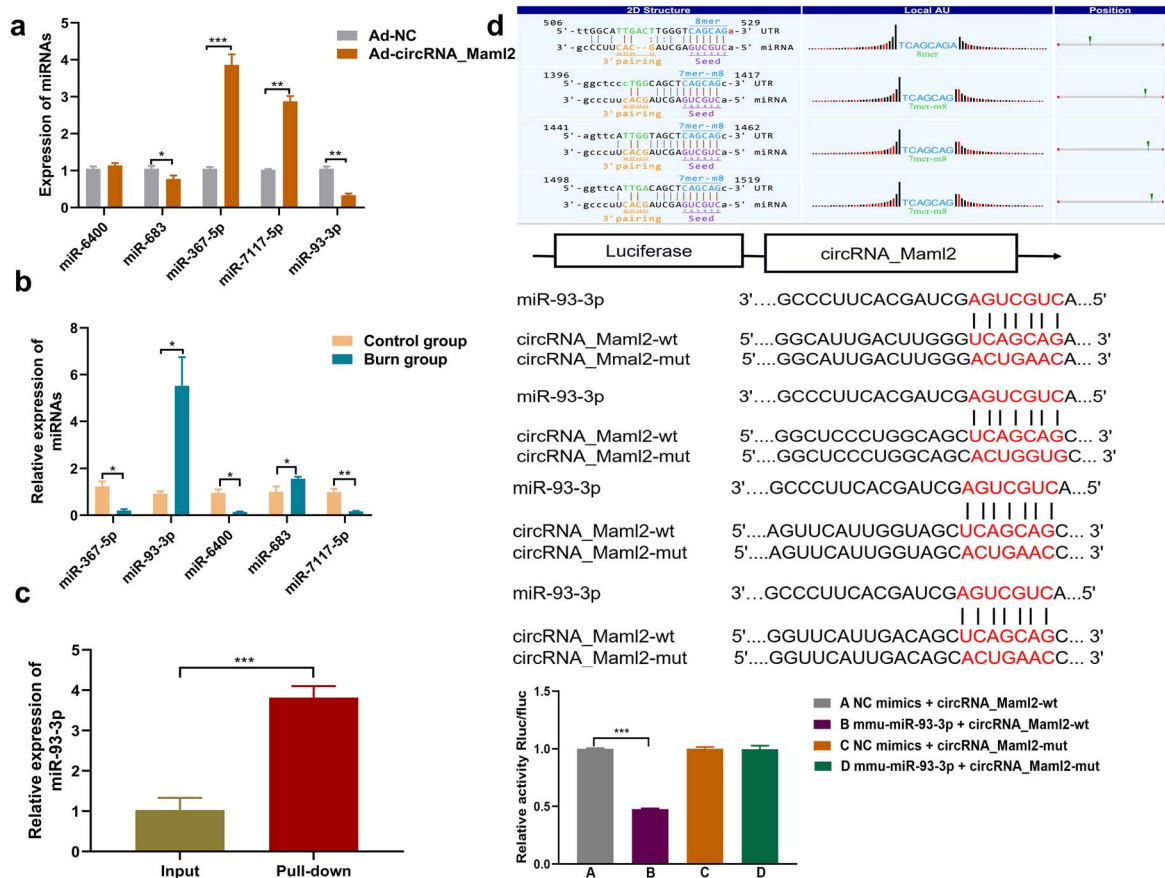


**Figure 4.** CircRNA\_Maml2 acts as a sponge for miR-93-3p in CT26.wt cells. (a) Expression of miRNAs after the overexpression of circRNA\_Maml2 was detected by qRT-PCR. (b) Expression of miRNAs in the intestinal tissues of mice after severe burns was detected by qRT-PCR. (c) miR-93-3p was pulled down by using a circRNA\_Maml2 with a specific biotinylated MS2 tag. (d) The binding sites of circRNA\_Maml2 and miR-93-3p were predicted by bioinformatics software. Schematic illustration of circRNA\_Maml2-WT and circRNA\_Maml2-Mut luciferase reporter vectors. Relative luciferase activities were investigated in CT26.wt cells after transfection with circRNA\_Maml2-WT or circRNA\_Maml2-Mut and miR-93-3p mimic or miR-NC. \* $p < 0.05$ , \*\* $p < 0.01$ , \*\*\* $p < 0.001$ . Ad adenovirus, WT wild type, Mut mutant, qRT-PCR quantitative real-time polymerase chain reaction

circRNA\_Maml2 may be reversed by miR-93-3p mimic. To understand whether circRNA\_Maml2 plays its biological role by regulating the expression of *Fzd7* by acting as the ceRNA of miR-93-3p, we designed a rescue experiment. The results showed that overexpression of circRNA\_Maml2 significantly up-regulated the expression of *Fzd7* mRNA and FZD7 protein, while co-transfection of circRNA\_Maml2 and miR-93-3p successfully reversed the increase in *Fzd7* expression caused by overexpression of circRNA\_Maml2 (Figure 6c, d). The results of the CCK-8 analysis demonstrated that the overexpression of circRNA\_Maml2 significantly promoted cell proliferation, while co-transfection of circRNA\_Maml2 and miR-93-3p significantly reversed the cell proliferation ability resulting from the promotion of circRNA\_Maml2 (Figure 6e). The results of EdU analysis results revealed that overexpression of circRNA\_Maml2 significantly enhanced the rate of increase of EdU-positive cells caused by overexpression of circRNA\_Maml2. On the other hand, the co-transfection of circRNA\_Maml2 and miR-93-3p significantly reversed the rate of increase of EdU-positive cells relative to

circRNA\_Maml2 promotion (Figure 6f). The findings from wound healing and transwell experiments showed that the overexpression of circRNA\_Maml2 significantly promoted cell migration, while co-transfection of circRNA\_Maml2 and miR-93-3p successfully reversed cell migration ability relative to the promotion of circRNA\_Maml2 (Figure 6g, h). In summary, these data indicate that circRNA\_Maml2 regulates the expression of *Fzd7* by competitively binding miR-93-3p, thereby promoting cell proliferation and migration and repair of damaged intestinal mucosa.

#### Overexpression of *Fzd7* promotes cell proliferation and migration

To decipher the biological role of *Fzd7* in promoting intestinal mucosal repair, we transfected the overexpression plasmid of *Fzd7* into CT26.wt cells to detect its effect on cell proliferation and migration. The findings shed light on the overexpression efficiency of *Fzd7* (Figure 7a). The results of CCK-8 analysis showed that up-regulation of *Fzd7* could

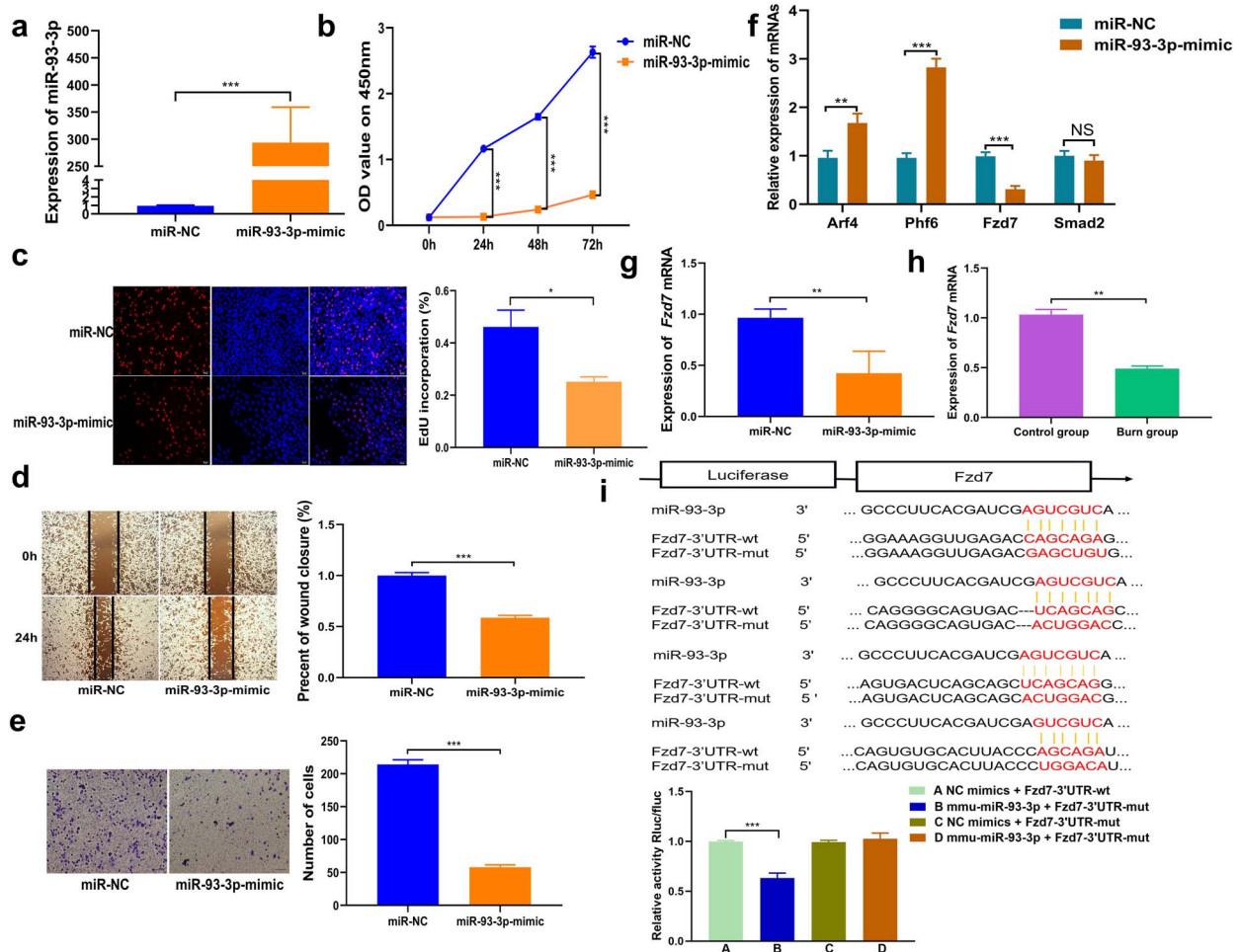


**Figure 5.** The function of miR-93-3p and FZD7 is the direct target of miR-93-3p. (a) Expression efficiency of miR-93-3p in CT26.wt cells transfected with mimic targeting miR-93-3p detected by qRT-PCR. (b) Growth curves of CT26.wt cells transfected with miR-93-3p mimic detected by the CCK-8 assay. (c) Number of EdU-positive CT26.wt cells transfected with miR-93-3p mimic detected by using EdU assay. (d, e) The migration ability of CT26.wt cells transfected with miR-93-3p mimic was detected by using wound healing experiment and transwell experiment. (f) Expression levels of *Arf4*, *Fzd7*, *Phf6* and *Smad2* after overexpression of miR-93-3p were detected by qRT-PCR. (g) Expression of *Fzd7* after the upregulation of miR-93-3p was detected by qRT-PCR. (h) Expression of *Fzd7* mRNA in the intestinal tissues of mice after severe burns was detected by qRT-PCR. (i) Schematic illustration of *Fzd7* 3'-UTR-WT and *Fzd7* 3'-UTR-Mut luciferase reporter vectors. Relative luciferase activities were investigated in CT26.wt cells after transfection with *Fzd7* 3'-UTR-WT or *Fzd7* 3'-UTR-Mut and miR-93-3p mimic or miR-NC. \* $p < 0.05$ , \*\* $p < 0.01$ , \*\*\* $p < 0.001$ . *Arf4* ADP ribosylation factor 4, *EdU* 5-ethynyl-2'-deoxyuridine, *Fzd7* frizzled class receptor 7, *Phf6*, PHD finger protein 6, *Smad2* SMAD family member 2, 3'-UTR 3' untranslated region, qRT-PCR quantitative real-time polymerase chain reaction

significantly promote cell proliferation (Figure 7b). The findings from EdU analysis revealed that the increased rate of EdU-positive cells was significantly augmented after upregulation of *Fzd7* (Figure 7c). The results of wound healing and transwell experiments showed that overexpression of *Fzd7* could significantly increase the migration ability of cells (Figure 7d, e). Studies have reported that FZD7 is a receptor for the Wnt signaling pathway and activates downstream signaling pathways by binding to Wnt ligands [22,23]. Interestingly, we found that the Wnt/ $\beta$ -catenin pathway was activated after FZD7 overexpression. To further explore the regulatory effect of FZD7 on downstream signaling pathways, we performed another rescue experiment. The vector-NC, miR-93-3p mimic, *Fzd7* overexpression

plasmid, and the miR-93-3p mimic and *Fzd7* overexpression plasmid were co-transfected into the CT26.wt cells. Western blotting results signified that the miR-93-3p mimic can significantly lower the protein level of  $\beta$ -catenin and vimentin, while co-transfection of miR-93-3p mimic and *Fzd7* overexpression plasmid could significantly offset the inhibitory effect of miR-93-3p mimic, in addition the miR-93-3p mimic could significantly increase the protein level of E-cadherin, while the co-transfection of miR-93-3p mimic and *Fzd7* overexpression plasmid could significantly offset the upregulation effect of miR-93-3p-mimic (Figure 7f). This result confirms that FZD7 could activate the downstream  $\beta$ -catenin signaling pathway to play an important biological role.

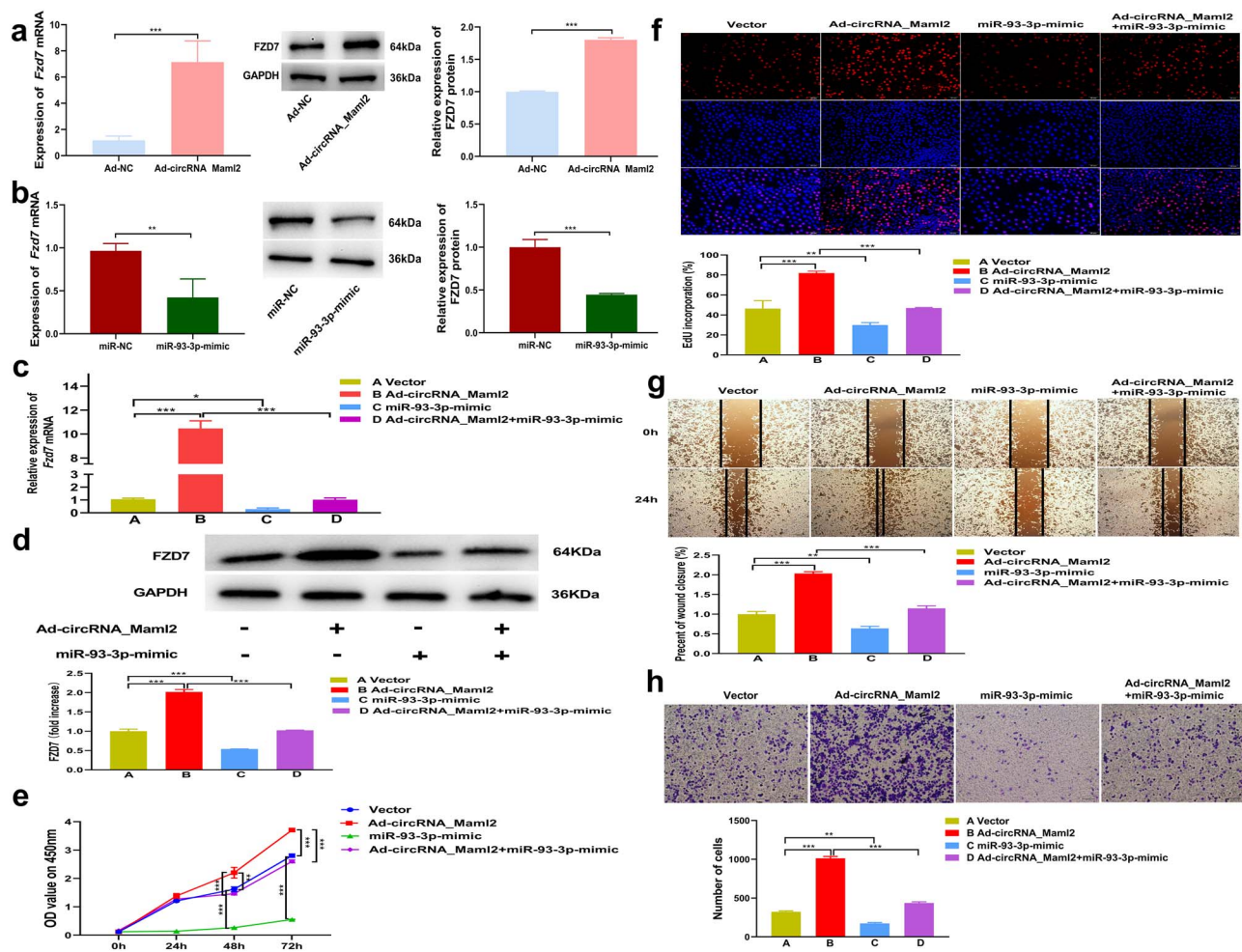


**Figure 6.** CircRNA\_Maml2 indirectly regulates Fzd7 through miR-93-3p. (a) Expression of *Fzd7* mRNA after the upregulation of circRNA\_Maml2 was detected by qRT-PCR. Expression of FZD7 protein after the upregulation of circRNA\_Maml2 was detected by western blot. (b) Expression of *Fzd7* mRNA after the upregulation of miR-93-3p was detected by qRT-PCR. Expression of FZD7 protein after the upregulation of miR-93-3p was detected by western blot. (c) Co-transfection of circRNA\_Maml2 and miR-93-3p successfully reversed the increase in *Fzd7* mRNA expression caused by the overexpression of circRNA\_Maml2. (d) The cotransfection of circRNA\_Maml2 and miR-93-3p successfully reversed the increase in FZD7 protein expression caused by the overexpression of circRNA\_Maml2. (e,f) CircRNA\_Maml2 and miR-93-3p significantly reversed the cell proliferation ability caused by the promotion of circRNA\_Maml2. (g,h) The co-transfection of circRNA\_Maml2 and miR-93-3p significantly reversed the cell migration ability caused by the promotion of circRNA\_Maml2. \* $p < 0.05$ , \*\* $p < 0.01$ , \*\*\* $p < 0.001$ . Ad adenovirus, EdU 5-ethynyl-2'-deoxyuridine, Fzd7 frizzled class receptor 7, GAPDH glyceraldehyde-3-phosphate dehydrogenase

### Up-regulation of circRNA\_Maml2 *in vivo* can promote the repair of damaged intestinal mucosa

To study the effect of circRNA\_Maml2 on damaged intestinal mucosa in severely burned mice, adenovirus overexpressing circRNA\_Maml2 was injected intraperitoneally into the gastrointestinal tract of mice before the construction of the severe burn model. The qRT-PCR results indicated that the expression of circRNA\_Maml2 decreased significantly after severe burns and that the expression increased significantly after intraperitoneal injection of the circRNA\_Maml2 adenovirus (Figure 8a). In addition, overexpression of circRNA\_Maml2 *in vivo* significantly inhibited the expression of miR-93-3p, while the mRNA and protein levels of *Fzd7* were obviously increased (Figure 8b-d). Light microscopy

findings signified that when compared with the control group, the intestinal mucosal injury in the burn group was more severe, the mucosal surface was severely congested and there was edema, the surface wall was thickened, or there was inflammation, and the score was higher. When compared with the burn group, the intestinal mucosal injury in the burn+Ad\_circRNA\_Maml2 group was lighter, with rough mucosa, hyperemia and edema, and the score was slightly lower (Figure 8e, Table 4). The results of HE staining revealed that the intestinal mucosal villi of the control group were neatly arranged, the epithelial cell layer was smooth and intact, and a thin layer of mucus was present on the surface of the intestinal mucosa. Conversely, the intestinal villi of the burn group were arranged in a



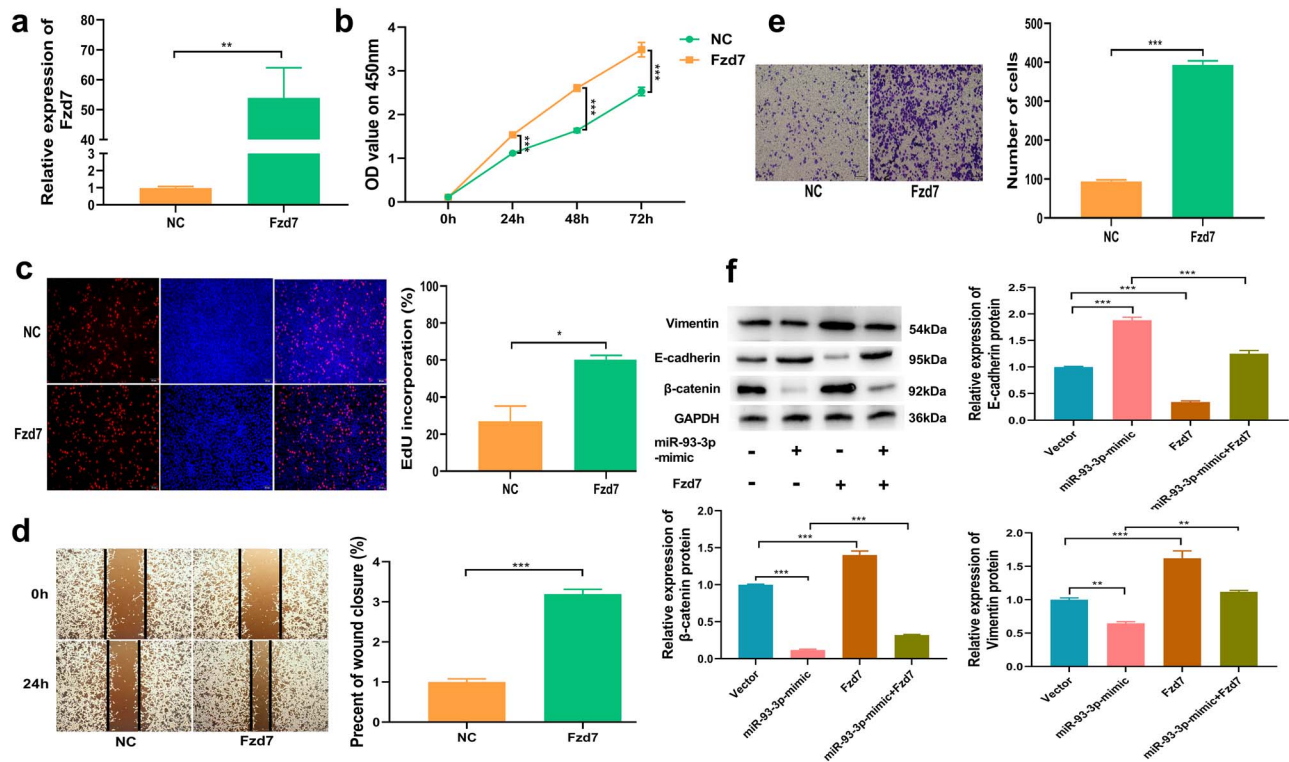


**Figure 7.** *Fzd7* promotes cell proliferation and migration. (a) Expression efficiency of *Fzd7* in CT26.wt cells transfected with plasmid targeting *Fzd7* detected by qRT-PCR. (b) Growth curves of CT26.wt cells transfected with *Fzd7* overexpression plasmid detected by the CCK-8 assay. (c) Number of EdU-positive CT26.wt cells transfected with *Fzd7* overexpression plasmid detected by the EdU assay. (d, e) The migration ability of CT26.wt cells transfected with *Fzd7* overexpression plasmid detected by using a wound healing experiment and the transwell experiment. (f)  $\beta$ -Catenin, vimentin and N-cadherin protein expression levels in the four groups of vector, miR-93-3p-mimic, *Fzd7*, miR-93-3p-mimic and *Fzd7* co-transfection. \* $p < 0.05$ , \*\* $p < 0.01$ , \*\*\* $p < 0.001$ . CCK-8 Cell counting kit-8, EdU 5-ethynyl-2'-deoxyuridine, *Fzd7* frizzled class receptor 7, GAPDH glyceraldehyde-3-phosphate dehydrogenase, qRT-PCR quantitative real-time polymerase chain reaction

**Table 4.** CMDI and Chiu scores of intestinal mucosal injury

Group	Control group	Burn group	Ad-circRNA_Maml2 + Burn group
CMDI scores	0.24 ± 0.08	3.08 ± 0.24***	2.15 ± 0.12###
Chiu's score	0.35 ± 0.11	3.07 ± 0.42***	2.08 ± 0.13###

Data are expressed as the mean ± standard deviation (SD),  $n = 10$ .

\*Represents a statistically significant difference in scores between the burn group and the control group.

#Represents a statistically significant difference in score between the burn group and the Ad-circRNA\_Maml2+ burn group.

\* $p < 0.05$ , \*\*\* $p < 0.001$ , # $p < 0.05$ , ### $p < 0.001$

CMDI Colonic Mucosa Damage Index, Ad adenovirus

disorderly manner and the epithelial cells exhibited edema and degeneration (or necrosis). Furthermore, a part of the villi was peeled off, leaving only the lamina propria. On the other hand, in the burn+Ad-circRNA\_Maml2 group the situation was relieved, i.e. the intestinal epithelial cell layer was relatively intact, with only congestion or edema and no large-scale bleeding, necrosis or shedding (Figure 8f, Table 3). In addition, we also measured the DAO level in the serum, which reflected the permeability of the intestinal mucosa after severe burns. The DAO results revealed that, when compared with the control group, the permeability of the

intestinal mucosa in the severe burn group was significantly increased. When compared with the severe burn group, the permeability of the intestinal mucosa of the burn+Ad-circRNA\_Maml2 group was reduced (Figure 8g). The findings of this *in vivo* study suggest that circRNA\_Maml2 may play a significant role in promoting the repair of damaged intestinal mucosa. Collectively, our results yet again prove that circRNA\_Maml2 regulates the expression of FZD7 by acting as a sponge for miR-93-3p and promoting the repair of damaged intestinal mucosa after severe burns.

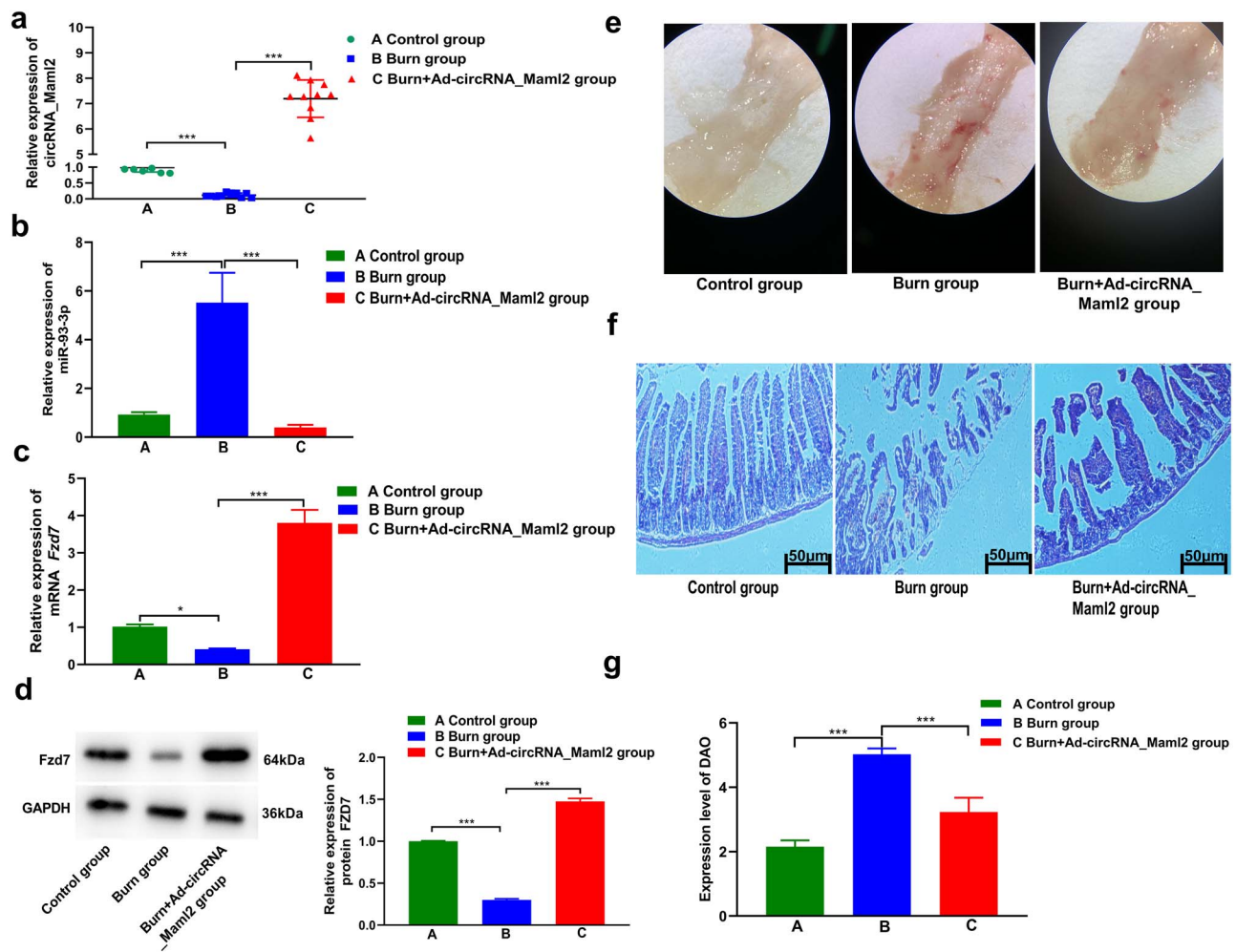


**Figure 8.** Upregulation of circRNA\_Maml2 promotes the repair of damaged intestinal mucosa after severe burns. (a) Expression of circRNA\_Maml2 was detected by qRT-PCR in the control group, burn group and burn+Ad-circRNA\_Maml2 group. (b) Expression of miR-93-3p was detected by qRT-PCR in the control group, burn group and burn+Ad-circRNA\_Maml2 group. (c, d) Expression of *Fzd7* mRNA and FZD7 protein was detected by qRT-PCR in the control group, burn group and burn+Ad-circRNA\_Maml2 group. (e) Injury of the intestinal mucosa under light microscope in the control group, burn group and burn+Ad-circRNA\_Maml2 group. (f) HE staining revealed the damage of the intestinal mucosa in the control group, burn group and burn+Ad-circRNA\_Maml2 group. (g) Expression level of DAO revealed the damage to the intestinal mucosa in the control group, burn group and burn+Ad-circRNA\_Maml2 group. \* $p < 0.05$ , \*\* $p < 0.01$ , \*\*\* $p < 0.001$ . Ad Adenovirus, *Fzd7* frizzled class receptor 7, qRT-PCR quantitative real-time polymerase chain reaction, U6 U6 small nuclear RNA, HE hematoxylin and eosin, DAO diamine oxidase

## Discussion

For a long time, people's interest in intestinal function was focused on the digestion and absorption of nutrients. As a result of several animal experiments and clinical studies, we have gained a good understanding of the intestinal barrier mechanism, mucosal metabolism and immune function [24]. Under normal conditions, the gastrointestinal tract depends on the defensive function of the gastrointestinal membrane barrier, which can protect the intestinal cavity from bacteria and endotoxins [25]. Acute gastrointestinal mucosal ischemia damage after severe burns and the resulting changes in gastrointestinal barrier function leads to systemic inflammatory response syndrome and multiple organ dysfunction syndromes after burns. Such issues further reduce the quality of burn shock resuscitation, induce enterogenous infections and serve as risk factors for endotoxemia [1,26]. Therefore,

understanding the molecular mechanism of gastrointestinal barrier dysfunction after burns, finding meaningful therapeutic targets and adopting effective therapeutic measures are of great significance in the management of severe burns.

CircRNA is a special type of non-coding RNA [27] formed by reverse splicing of pre-mRNA transcripts [28]. The 5'-end and 3'-end of circRNA are connected to form a closed loop. This type of RNA has no 5' end-cap structure or 3' poly (A) tail, which makes circRNA resistant to degradation by ribonuclease. Hence, circRNA can maintain stable intracellular expression [29,30]. Owing to its unique structure, circRNA is very stable in mammals, highly conserved in evolution, and has certain tissue and time specificities in terms of expression [31]. In recent years, with the development of RNA purification technologies, bioinformatics analysis,



high-throughput RNA sequencing technology and various circRNA research tools, >30,000 circRNAs have been discovered. They are widely distributed in eukaryotic organisms [15]. At present, based on the differences in the biogenesis patterns of the genome, circRNA can be divided into four subtypes: exon circRNA composed of exon sequences; intron RNA composed of intron sequences; exon and intron circRNA composed of subsequences; and intergenic circRNA composed of sequences within the breakpoints between the genes [32]. The most common and important function of circRNA is to act as a miRNA sponge. circRNAs and miRNAs have the strongest binding ability among the ceRNAs. They act as miRNA molecular sponges in cell gene expression and regulate the translation and expression of proteins, thereby controlling the occurrence and development of many diseases. For example, circMTO1 acts as a sponge for microRNA-9 to inhibit the progression of hepatocellular carcinoma [33] and circNRIP1 acts as a microRNA-149-5p sponge to promote the progression of gastric cancer through the AKT1/mTOR pathway [34]. It has been shown that circRNA protects the heart from pathological hypertrophy and failure by targeting miR-223 [35]. Moreover, circRNAs can directly regulate the expression level of other RNAs through base complementary pairing and combine with RNA binding proteins (RBPs) to regulate protein functions, such as combining transcription factors to inhibit gene transcription. Studies have reported that the knock-out of circRNA-RasGEF1B in macrophages leads to a decrease in the expression of lipopolysaccharide-induced intercellular adhesion molecule-1, which is achieved by regulating the stability of intercellular adhesion molecule-1 [36]. However, whether the circRNA expression profile of the intestinal mucosa changes after severe burns and whether circRNA can promote repair of damaged intestinal mucosa remains unclear.

In previous studies, we screened the circRNA expression profile in the intestinal tissues of mice after severe burns using circRNA microarray data [11]. Subsequently, we identified a circRNA with the highest down-regulation factor, namely circRNA\_Maml2, which originated from the second exon of Maml2 and formed an end-to-end closed circRNA. Furthermore, we confirmed the existence of circRNA\_Maml2. The divergent primers were able to amplify circRNA in cDNA but not in gDNA. After RNaseR treatment, circRNA\_Maml2 resisted digestion, while most of the host genes of circRNA\_Maml2 were digested. Additionally, the nucleoplasmic separation experiment revealed that circRNA\_Maml2 was located in the cytoplasm. Further experimental results suggested that the overexpression of circRNA\_Maml2 *in vitro* significantly promoted cell proliferation and migration and overexpression of circRNA\_Maml2 *in vivo* promoted the repair of damaged intestinal mucosa. These results imply that circRNA\_Maml2 plays an important role in the damage and repair of intestinal mucosa in mice after severe burns. Reports on the ceRNA hypothesis indicated that circRNA, lncRNA, pseudogenes and mRNA can usually competitively bind to MRE and further regulate mRNA expression and

translation. Studies have shown that Circ\_0002770, as a ceRNA, promotes cell proliferation and invasion by targeting miR-331-3p in melanoma [37]. To test whether circRNA\_Maml2 works through the ceRNA mechanism, the pull-down experiment and the dual luciferase reporter gene experiment were performed. The results confirmed that miR-93-3p was the target of circRNA\_Maml2 and that the two can directly interact with each other. In addition, the expression of miR-93-3p in the intestinal tissues of mice increased significantly after severe burns and the expression of miR-93-3p decreased significantly after the overexpression of circRNA\_Maml2. Besides, the up-regulation of miR-93-3p successfully reversed the effects of cell proliferation and migration caused by circRNA\_Maml2. Our results suggest that circRNA\_Maml2 could act as a sponge for miR-93-3p, and the two interact with each other to promote the repair of damaged intestinal mucosa.

Bioinformatics analysis predicted that FZD7 was a potential target of miR-93-3p. When miR-93-3p was up-regulated, mRNA and protein expression levels of *Fzd7* were significantly lowered. Moreover, the dual luciferase reporter gene experiments proved that miR-93-3p bound to the 3'-UTR of *Fzd7* to regulate it. In addition, we found that FZD7 was down-regulated in the intestinal tissue of severely burned mice. FZD7 is a 7-pass transmembrane cell surface receptor, a new member of the G protein-coupled receptor family, and a key factor in the Wnt signaling pathway [22]. FZD7 combines with Wnt ligands to activate canonical or non-canonical Wnt signaling pathways and mainly regulates cell proliferation, differentiation, migration and tumor occurrence and development [38]. Studies have demonstrated that FZD7 is significantly up-regulated in colon cancer cell lines and can activate the classic Wnt pathway in these cells, thereby leading to progression of the disease [39]. We identified that the forced expression of FZD7 can increase the protein expression of  $\beta$ -catenin. This finding suggests that FZD7 can activate the Wnt/ $\beta$ -catenin signaling pathway, thereby regulating cell proliferation and migration and promoting intestinal mucosal repair. The results from this series of studies support our hypothesis that circRNA\_Maml2 acts as a ceRNA to absorb miR-93-3p and activate the FZD7-mediated Wnt/ $\beta$ -catenin signaling pathway, thereby promoting cell proliferation and migration and aiding in the repair of damaged intestinal mucosa after severe burns.

These findings confirm that circRNA\_Maml2 promotes cell proliferation and migration, thereby promoting the repair of damaged intestinal mucosa.

## Conclusions

In conclusion, we have established that circRNA\_Maml2 is significantly down-regulated in the intestinal tissues of mice after severe burns and that it is related to the repair of damaged intestinal mucosa. Our findings have further proven that circRNA\_Maml2 acts as a sponge adsorption molecule for miR-93-3p to regulate the expression of FZD7, activates

the Wnt/ $\beta$ -catenin signaling pathway and promotes the repair of damaged intestinal mucosa after severe burns. Based on these results, circRNA\_Maml2 is expected to become a therapeutic target for the treatment of damaged intestinal mucosa.

## Abbreviations

Ad: Adenovirus; Arf4: ADP ribosylation factor 4; CCK-8: cell counting kit-8; ceRNA: competitive endogenous RNA; circRNA: circular RNA; DAO: diamine oxidase; EdU: 5-ethynyl-2'-deoxyuridine; FISH: Fluorescence in situ hybridization; Fzd7: frizzled class receptor 7; GAPDH: glyceraldehyde-3-phosphate dehydrogenase; HE: hematoxylin and eosin; miRNA: microRNA; MRE: miRNA response element; Phf6: PHD finger protein 6; RBPs: RNA binding proteins; qRT-PCR: quantitative real-time polymerase chain reaction; Smad2: SMAD family member 2; U6: U6 small nuclear RNA; 3'-UTR: 3' untranslated region.

## Acknowledgments

Thanks to Hanbio Biotechnology Co. Ltd (Shanghai, China) and Guangzhou Jisai Biological Company (Guangzhou, China) for their technical support and consultation. Thanks for the animals provided by Animal Experiment Center of Xuzhou Medical University (Xuzhou, China). The authors would like to thank all the reviewers who participated in the review and Mjeditor ([www.mjeditor.com](http://www.mjeditor.com)) for linguistic assistance during the preparation of this manuscript. Thanks to all the authors for their contributions.

## Funding

This work was supported by the National Natural Science Foundation of China (81772082), the Natural Science Foundation of Jiangsu Province (BK20211060), the Natural Science Foundation of Xuzhou (KC20085) and the Postgraduate Innovation Program of Jiangsu Province (KYCX20\_2484).

## Authors' contributions

W.W.Z., Y.L., J.Q.L., M.M.Z. and Y.S. designed the experiments. W.W.Z. and Y.L. conducted the experiments. W.W.Z., J.Q.L., Y.L. and Q.L. interpreted and analyzed the data. W.W.Z., H.Y., Y.Q.D., J.Q.L., Q.L. and Y.L. contributed to literature search/analysis tools. W.W.Z. and Y.S. made critical revisions. W.W.Z. wrote the article. W.W.Z., X.H.X. and D.D.W. analyzed statistical methods.

## Ethics approval and consent to participate

The human studies were approved by the Medical and Ethics Committee of Huahai Hospital Affiliated with Xuzhou Medical University. The process number for human experiments is: 2018–002. The animal studies were examined and verified by

the Laboratory Animal Ethics Committee of Xuzhou Medical University following the Guide to Laboratory Animal Ethics Examination of Xuzhou Medical University. The relevant animal experiments are permitted. The process number for animal experiments is: 202010 W001.

## Conflict of interest

None declared.

## References

1. Wilmore DW, Smith RJ, O'Dwyer ST, Jacobs DO, Ziegler TR, Wang XD. The gut: a central organ after surgical stress. *Surgery*. 1988;104:917–23.
2. Porter C, Tompkins RG, Finnerty CC, Sidossis LS, Suman OE, Herndon DN. The metabolic stress response to burn trauma: current understanding and therapies. *Lancet*. 2016;388:1417–26.
3. Zhuang M, Deng Y, Zhang W, Zhu B, Yan H, Lou J, et al. LncRNA Bmp1 promotes the healing of intestinal mucosal lesions via the miR-128-3p/PHF6/PI3K/AKT pathway. *Cell Death Dis*. 2021;12:595.
4. Magnotti LJ, Deitch EA. Burns, bacterial translocation, gut barrier function, and failure. *J Burn Care Rehabil*. 2005;26:383–91.
5. Li C, Li Y, Zhuang M, Zhu B, Zhang W, Yan H, et al. Long noncoding RNA H19 act as a competing endogenous RNA of let-7g to facilitate IEC-6 cell migration and proliferation via regulating EGF. *J Cell Physiol*. 2021;236:2881–92.
6. Li X, Yang L, Chen LL. The biogenesis, functions, and challenges of circular RNAs. *Mol Cell*. 2018;71:428–42.
7. Sanger HL, Klotz G, Riesner D, Gross HJ, Kleinschmidt AK. Viroids are single-stranded covalently closed circular RNA molecules existing as highly base-paired rod-like structures. *Proc Natl Acad Sci U S A*. 1976;73:3852–6.
8. Cocquerelle C, Mascrez B, Hetuin D, Bailleul B. Mis-splicing yields circular RNA molecules. *FASEB J*. 1993;7:155–60.
9. Arnaiz E, Sole C, Manterola L, Iparraguirre L, Otaegui D, Lawrie CH. CircRNAs and cancer: biomarkers and master regulators. *Semin Cancer Biol*. 2019;58:90–9.
10. Li P, Chen S, Chen H, Mo X, Li T, Shao Y, et al. Using circular RNA as a novel type of biomarker in the screening of gastric cancer. *Clin Chim Acta*. 2015;444:132–6.
11. Zhang W, Yan H, Deng Y, Lou J, Zhang P, Cui Q, et al. Expression profile and bioinformatics analysis of circular RNA in intestinal mucosal injury and repair after severe burns. *Cell Biol Int*. 2020;44:2570–87.
12. Jinek M, Doudna JA. A three-dimensional view of the molecular machinery of RNA interference. *Nature*. 2009;457:405–12.
13. Salmena L, Poliseno L, Tay Y, Kats L, Pandolfi PP. A ceRNA hypothesis: the Rosetta stone of a hidden RNA language? *Cell*. 2011;146:353–8.
14. Wang Y, Juranek S, Li H, Sheng G, Tuschl T, Patel DJ. Structure of an argonaute silencing complex with a seed-containing guide DNA and target RNA duplex. *Nature*. 2008;456:921–6.
15. Memczak S, Jens M, Elefsinioti A, Torti F, Krueger J, Rybak A, et al. Circular RNAs are a large class of animal RNAs with regulatory potency. *Nature*. 2013;495:333–8.
16. Zhang DY, Qiu W, Jin P, Wang P, Sun Y. Role of autophagy and its molecular mechanisms in mice intestinal tract after severe burn. *J Trauma Acute Care Surg*. 2017;83:716–24.

17. Ahmad A, Druzhyina N, Szabo C. Cystathionine-gamma-lyase deficient mice are protected against the development of multiorgan failure and exhibit reduced inflammatory response during burn. *Burns*. 2017;43:1021–33.
18. Chen C, Wang P, Su Q, Wang S, Wang F. Myosin light chain kinase mediates intestinal barrier disruption following burn injury. *PLoS One*. 2012;7:e34946.
19. Wang L, Yang G, Zhu X, Wang Z, Wang H, Bai Y, *et al*. miR-93-3p inhibition suppresses clear cell renal cell carcinoma proliferation, metastasis and invasion. *Oncotarget*. 2017;8: 82824–34.
20. Feng Z, Chen R, Huang N, Luo C. Long non-coding RNA ASMTL-AS1 inhibits tumor growth and glycolysis by regulating the miR-93-3p/miR-660/FOXO1 axis in papillary thyroid carcinoma. *Life Sci*. 2020;244:117298.
21. Li C, Wang F, Wei B, Wang L, Kong D. LncRNA AWPPH promotes osteosarcoma progression via activation of Wnt/beta-catenin pathway through modulating miR-93-3p/FZD7 axis. *Biochem Biophys Res Commun*. 2019;514:1017–22.
22. MacDonald BT, Tamai K, He X. Wnt/beta-catenin signaling: components, mechanisms, and diseases. *Dev Cell*. 2009;17:9–26.
23. Fernandez A, Huggins IJ, Perna L, Brafman D, Lu D, Yao S, *et al*. The WNT receptor FZD7 is required for maintenance of the pluripotent state in human embryonic stem cells. *Proc Natl Acad Sci U S A*. 2014;111:1409–14.
24. He W, Wang Y, Wang P, Wang F. Intestinal barrier dysfunction in severe burn injury. *Burns Trauma*. 2019;7:24.
25. Lachiewicz AM, Hauck CG, Weber DJ, Cairns BA, van Duin D. Bacterial infections after burn injuries: impact of multidrug resistance. *Clin Infect Dis*. 2017;65:2130–6.
26. Udy AA, Roberts JA, Lipman J, Blot S. The effects of major burn related pathophysiological changes on the pharmacokinetics and pharmacodynamics of drug use: an appraisal utilizing antibiotics. *Adv Drug Deliv Rev*. 2018;123: 65–74.
27. Chen B, Huang S. Circular RNA: an emerging non-coding RNA as a regulator and biomarker in cancer. *Cancer Lett*. 2018;418:41–50.
28. Qu S, Yang X, Li X, Wang J, Gao Y, Shang R, *et al*. Circular RNA: a new star of noncoding RNAs. *Cancer Lett*. 2015;365:141–8.
29. Lasda E, Parker R. Circular RNAs: diversity of form and function. *RNA*. 2014;20:1829–42.
30. Suzuki H, Tsukahara T. A view of pre-mRNA splicing from RNase R resistant RNAs. *Int J Mol Sci*. 2014;15:9331–42.
31. Salzman J, Chen RE, Olsen MN, Wang PL, Brown PO. Cell-type specific features of circular RNA expression. *PLoS Genet*. 2013;9:e1003777.
32. Holdt LM, Kohlmaier A, Teupser D. Molecular roles and function of circular RNAs in eukaryotic cells. *Cell Mol Life Sci*. 2018;75:1071–98.
33. Han D, Li J, Wang H, Su X, Hou J, Gu Y, *et al*. Circular RNA circMTO1 acts as the sponge of microRNA-9 to suppress hepatocellular carcinoma progression. *Hepatology*. 2017;66:1151–64.
34. Zhang X, Wang S, Wang H, Cao J, Huang X, Chen Z, *et al*. Circular RNA circNRIP1 acts as a microRNA-149-5p sponge to promote gastric cancer progression via the AKT1/mTOR pathway. *Mol Cancer*. 2019;18:20.
35. Wang K, Long B, Liu F, Wang JX, Liu CY, Zhao B, *et al*. A circular RNA protects the heart from pathological hypertrophy and heart failure by targeting miR-223. *Eur Heart J*. 2016;37:2602–11.
36. Ng WL, Marinov GK, Chin YM, Lim YY, Ea CK. Transcriptomic analysis of the role of RasGEF1B circular RNA in the TLR4/LPS pathway. *Sci Rep*. 2017;7:12227.
37. Qian P, Linbo L, Xiaomei Z, Hui P. Circ\_0002770, acting as a competitive endogenous RNA, promotes proliferation and invasion by targeting miR-331-3p in melanoma. *Cell Death Dis*. 2020;11:264.
38. Simonetti M, Agarwal N, Stosser S, Bali KK, Karaulanov E, Kamble R, *et al*. Wnt-Fzd signaling sensitizes peripheral sensory neurons via distinct noncanonical pathways. *Neuron*. 2014;83:104–21.
39. Ueno K, Hiura M, Suehiro Y, Hazama S, Hirata H, Oka M, *et al*. Frizzled-7 as a potential therapeutic target in colorectal cancer. *Neoplasia*. 2008;10:697–705.